PHILOSOPHICAL TRANSACTIONS B

rstb.royalsocietypublishing.org

Research

Cite this article: Burdine RD, Grimes DT. 2016 Antagonistic interactions in the zebrafish midline prior to the emergence of asymmetric gene expression are important for left–right patterning. *Phil. Trans. R. Soc. B* **371**: 20150402.
http://dx.doi.org/10.1098/rstb.2015.0402

Accepted: 12 September 2016

One contribution of 17 to a theme issue 'Provocative questions in left–right asymmetry'.

Subject Areas:
developmental biology

Keywords:
Nodal, Lefty, one-eyed pinhead, EGF-CFC, asymmetry, zebrafish

Author for correspondence:
Rebecca D. Burdine
e-mail: rburdine@princeton.edu

Electronic supplementary material is available online at https://dx.doi.org/10.6084/m9.figshare.c.3515250.

THE ROYAL SOCIETY PUBLISHING

Antagonistic interactions in the zebrafish midline prior to the emergence of asymmetric gene expression are important for left–right patterning

Rebecca D. Burdine and Daniel T. Grimes

Department of Molecular Biology, Princeton University, Princeton, NJ 08544, USA

RDB, 0000-0001-6620-5015

Left–right (L-R) asymmetry of the internal organs of vertebrates is presaged by domains of asymmetric gene expression in the lateral plate mesoderm (LPM) during somitogenesis. Ciliated L-R coordinators (LRCs) are critical for biasing the initiation of asymmetrically expressed genes, such as *nodal* and *pitx2*, to the left LPM. Other midline structures, including the notochord and floorplate, are then required to maintain these asymmetries. Here we report an unexpected role for the zebrafish EGF-CFC gene *one-eyed pinhead* (*oep*) in the midline to promote *pitx2* expression in the LPM. Late zygotic *oep* (LZ*oep*) mutants have strongly reduced or absent *pitx2* expression in the LPM, but this expression can be rescued to strong levels by restoring *oep* in midline structures only. Furthermore, removing midline structures from LZ*oep* embryos can rescue *pitx2* expression in the LPM, suggesting the midline is a source of an LPM *pitx2* repressor that is itself inhibited by *oep*. Reducing *lefty1* activity in LZ*oep* embryos mimics removal of the midline, implicating *lefty1* in the midline-derived repression. Together, this suggests a model where Oep in the midline functions to overcome a midline-derived repressor, involving *lefty1*, to allow for the expression of left side-specific genes in the LPM.

This article is part of the themed issue 'Provocative questions in left–right asymmetry'.

1. Introduction

(a) Nodal signalling in left–right patterning

Left–right (L–R) patterning in the vertebrate embryo emerges as genes become asymmetrically expressed during somitogenesis. Genes encoding components of the Nodal signalling pathway, including the *nodal* ligand and the downstream target *pitx2*, are expressed in the left lateral plate mesoderm (LPM) but remain absent from the right side (reviewed in [1–5]). Nodal is a transforming growth factor-beta (TGF-β) superfamily member that signals through serine/threonine kinase receptors to phosphorylate Smad2 and Smad3 (reviewed in [6,7]). This requires EGF-CFC proteins, such as that encoded by the zebrafish gene *one-eyed pinhead* (*oep*), which act as co-receptors for Nodal ligands [8–11]. Smad2 and Smad3 then interact with the co-Smad, Smad4, as well as transcription factors, such as FoxHI, to induce transcription of downstream targets [12–18]. These targets include the asymmetrically expressed genes *pitx2*, *nodal* itself and the *lefty* repressors that restrict the extent of Nodal signalling. Owing to the feedback nature of the pathway, *lefty* expression denotes both areas where Nodal signalling has occurred and areas where Nodal signalling is now being repressed (reviewed in [6,7]). Lefty is thought to repress Nodal signals by physically associating with both Nodal itself as well as with EGF-CFC co-receptors including Oep [8,10,11].

Prior to the emergence of *nodal* expression in the left LPM, *nodal* is expressed at the midline around so-called left–right coordinators (LRCs). These are the

ventral node in mouse embryos [19], the gastrocoel roof plate in *Xenopus laevis* [20], and Kupffer's vesicle (KV) in zebrafish and Medaka fish [21–23]. Some evidence, including phenotypes of hypomorphic- or tissue-specific knock-out alleles of *Nodal* in the mouse, suggests that Nodal ligand emanating from this LRC domain is required for initiation of *Nodal* expression in the LPM [24–28]. In zebrafish, knockdown of the Nodal orthologue *southpaw* (*spaw*) results in a loss of *spaw* expression in the LPM, although transcription of *spaw* around the zebrafish LRC is unaffected [29]. Together, this suggests that LRC–Nodal activity induces expression of LPM–*nodal*. Subsequently, Nodal spreads throughout the left LPM and induces other asymmetrically expressed genes.

Further support for an essential role of Nodal signalling in inducing asymmetric expression in the LPM comes from the analysis of mutations in the EGF-CFC genes *oep* in zebrafish and *Cryptic*/*Cfc1* in mouse. These genes are expressed bilaterally in the LPM, and in the embryonic midline and its precursors [30,31]. *Cryptic* mutants lack expression of *Nodal*, *Lefty2*, and *Pitx2* in the LPM, and have organ laterality defects including right pulmonary isomerism and randomization of heart looping [32,33]. Similarly, zebrafish *oep* is required for L–R patterning. Maternal-zygotic *oep* (MZ*oep*) mutants lack most mesendoderm [9]. This early requirement for *oep* in Nodal signalling is rescued by *oep* mRNA injection into 1-cell stage embryos, generating 'late zygotic' *oep* (LZ*oep*) embryos [9,33]. These embryos are fully viable and develop to adulthood. All major structures and organs, ranging from midline and central nervous system to heart and pancreas, appear morphologically normal. However, as *oep* activity in later development is not provided by injected mRNA, LZ*oep* mutants have L–R patterning defects [33]; they do not express *nodal*/*cyclops* or *pitx2* in the LPM nor in an additional asymmetric expression domain in the dorsal diencephalon [33–35]. LZ*oep* mutants also display a randomization of heart looping and pancreas positioning in the viscera, and of parapineal positioning in the brain [33,34]. The importance of EGF-CFC genes in L–R development also extends to humans, as *CFC1* mutations are associated with human L–R patterning defects [36].

How Nodal signals are transferred from LRC to LPM is not fully understood. One possibility is that Nodal ligand directly travels from the lateral edges of the LRC to the LPM, a process that requires sulfated glycosaminoglycans (sGAGs; [27,37]). Moreover, Ca^{2+} signals are also observed around LRCs [38–40], and these signals can spread laterally towards the LPM via gap junctions [41,42]. Indeed, it has been hypothesized that Ca^{2+} signals aid in the transduction of Nodal ligand from LRC to LPM by inducing the secretion of sGAGs [41,43,44].

(b) Roles for midline structures in initiating and maintaining L–R asymmetries

Although the striking domain of asymmetric gene expression occurs in the LPM, various midline structures are critical for both initiating and maintaining these asymmetries. In vertebrates, a major model for how L–R asymmetries are initiated involves an asymmetric fluid flow within LRCs, driven by the rotation of polarized motile cilia [19,20,23,45–53]. In support of this model, a plethora of mutants that exhibit cilia motility abnormalities also display defects of L–R patterning (for just a few examples see [54–58]). How asymmetric fluid flow is sensed by the embryo to drive downstream asymmetries in gene expression around LRCs is not fully understood, but the process likely involves both sensory cilia and the polycystin transmembrane proteins Pkd1l1 and Pkd2 [39,59–67]. Downstream of fluid flow and Polycystin function, R > L asymmetries in *Dand5* (also called *charon* in zebrafish and Medaka, *Cerl2* in mouse and *Coco* in *Xenopus*), a member of the DAN family of Nodal inhibitors, emerge at the lateral edges of LRCs [28,68–75]. This results in more active Nodal emanating from the left side of LRCs and, presumably as a result, the activation of *Nodal* preferentially in the left LPM. As such, asymmetries in *Dand5* are critical for establishing unilateral left-sided *Nodal* expression in various vertebrate embryos.

Once asymmetric gene expression is established in the LPM, midline structures are also critical for maintaining asymmetries. Initial analysis of zebrafish mutants, in which an intact notochord fails to form, revealed defects in asymmetric gene expression in the LPM with subsequent abnormalities in cardiac asymmetry [76–78]. Similar results were obtained upon extirpation of midline structures in *Xenopus* [76,79]. In embryos without intact midline structures, gene expression normally restricted to the left side becomes bilaterally expressed in the left and right LPM. Based on these results, the midline (predominantly notochord and floorplate) was proposed to act as a barrier in L–R patterning. In the barrier model, the midline would act to prevent Nodal activity within the left LPM from accessing the right LPM, which remains capable of expressing *nodal*. The barrier activities of the midline would be perturbed upon loss of midline structures, allowing Nodal signals from the left access to the right LPM, resulting in bilateral expression of left side-specific genes.

Bilateral expression of *pitx2* and other genes in the LPM is also seen upon loss of *lefty1* function in mouse and zebrafish [80,81]. *lefty1* is expressed in the floorplate of mouse embryos and in the notochord in zebrafish [82–84] and has been proposed to act as the molecular component of the midline that restricts Nodal signalling to the left side. In mouse, *Lefty1* is induced in the midline by Nodal signals from the left LPM, and may thus serve as a barrier to Nodal signals preventing their access to the right LPM [85]. Many results pertaining to the barrier/repressor function of the midline were synthesized into a self-enhancement and lateral-inhibition (SELI) model in the mouse embryo [86]. In this model, *Nodal* is induced in both the left and right LPM, though at a much lower level in the latter. Thus, the critical threshold for robust activation and spreading (the self-enhancement) is not reached in the right LPM as it is in the left. Left LPM Nodal induces *Lefty* in both the left LPM and midline and these repressive signals raise the threshold for Nodal enhancement in the right LPM (the lateral inhibition), thereby maintaining unilateral expression. In the absence of Lefty repressors, Nodal is more strongly induced in the right LPM and, moreover, Nodal signals might also spread from the left LPM to the right LPM, ultimately resulting in bilateral expression of *Nodal* signals even in the presence of correct initial symmetry breaking at the LRC.

In addition to the floorplate/notochord *lefty* barrier, two additional 'midline barriers' that also involve repression of Nodal signals have been described in zebrafish [80]. Zebrafish expression of Nodal/Spaw in the LPM induces its own expression, but in contrast with mouse, does not induce the expression of *lefty* in the LPM. Instead, *lefty1* expression in the notochord is driven by Spaw as it propagates anteriorly within the LPM at these stages [87,88]). *lefty2* is induced within the left side of the heart field once Spaw reaches the

anterior left LPM [80]. Removal of *lefty2* from embryos allows *spaw* expression from the left anterior LPM to proceed across the region anterior to the notochord, into the right LPM, where it proceeds towards the posterior. This demonstrates that *lefty2* expression in the heart prevents *spaw* expression from spreading from the left to the right LPM. Similarly, bone morphogenetic protein (BMP) signalling is required to prevent Spaw in the left LPM from inducing *spaw* expression in a domain posterior to KV. In the absence of BMP signalling, *spaw* is ectopically expressed throughout the posterior LPM around the tailbud, and from there spreads to the right LPM. Thus, along with *lefty1* expression in the notochord, these two 'barriers' confine *nodal*/*spaw* expression to the left LPM from an area lateral to KV to an area lateral to the anterior notochord in zebrafish [80].

Current models suggest that the midline is essentially passive, responding to Nodal signals from the LPM by expressing *lefty1* and then preventing Nodal signals from activating in the right LPM. However, *lefty1* expression in the posterior notochord in zebrafish begins prior to the expression of *nodal* in the LPM, demonstrating that this domain of *lefty1*, whose function is currently unknown, cannot be initiated by Nodal signals from the LPM. Based on the results reported here, we propose that this early domain of *lefty1* contributes to establishing the threshold required for Nodal signals to initiate and propagate in the LPM. We demonstrate an active role for the Nodal co-receptor Oep in repressing early Lefty activity in the midline, prior to the emergence of asymmetric gene expression, to allow for expression of the Nodal target *pitx2* in the LPM.

2. Material and methods

(a) Zebrafish

Danio rerio strains were raised under standard conditions at 28°C. We used the PWT strain for experiments as this strain was found to have a very low level of abnormal asymmetric gene expression [60]. Transplanted and injected embryos were raised at 28°C until shield stage and then placed at 25°C overnight. The next morning, embryos were returned to 28°C until they reached 18–20 somites, when they were fixed for *in situ* analysis. All embryos were staged according to [89]. The oep^{tz257} mutant was used in this study [90–93].

(b) RNA and morpholino injections

Capped mRNA transcripts were synthesized using Ambion mMessage mMachine™ kits and quantitated by UV spectrophotometry. *oep* mRNA was transcribed from plasmid pJZoepFlag1–2 linearized with SmaI [31]. Morpholino antisense oligos were obtained from GeneTools, LLC and resuspended to a stock concentration of 50 μg μl^{-1} in dH_2O. The *ntla* morpholino sequence we used in these studies is described in [94]. The *lefty1* morpholino used is described in [95]. RNA and morpholinos were diluted in 5 mg ml^{-1} phenol red dissolved in 0.2 M KCl to concentrations that would deliver the desired amount in 100–500 pl injection volumes. Injection volumes were calibrated by micrometer as described [9]. RNA and morpholinos were microinjected into dechorionated embryos at the 1–2 cell stage. Concentrations injected per embryo were as follows: *oep* RNA 50 pg, *ntla* morpholino 200 or 400 pg, *lefty1* morpholino 250 pg and control morpholino 250 pg. Note, these experiments were conducted in early 2000s and the preparation of morpholinos at that time allowed for clean phenocopies at very low concentrations. Today, we typically use 2 ng or more of these same morpholinos to produce the same effect. To generate LZ*oep* embryos, *oep* RNA was injected into 1–2 cell stage embryos derived from crossing adults homozygous for the oep^{tz257} mutation.

(c) Shield transplantations and ablations

To label donor cells, donor embryos were injected with lysine fixable fluorescein dextran 10 000 MW dye (Molecular Probes) resuspended at 5% w/v in 5 mg ml^{-1} phenol red dissolved in 0.2 M KCl. For transplantation, donor embryos were injected with 500 pl fluorescein dextran alone or containing the appropriate amount of RNA or morpholino as described above. Shield transplantations and ablations were done as described [96]. Transplantations and ablations were performed in either 1× Danieau as described [96], or in Hank's balanced salt solution. Any transplanted embryos that did not develop normally were omitted from analysis. For example, embryos with abnormal bends or kinks in the axis, abnormal extension of the axis, or embryos with any degree of cyclopia were omitted. In embryos containing shield transplants, labelling of some dorsal spinal cord neurons was occasionally observed [97], but any embryos with substantial labelling outside of axial mesoderm derivatives were omitted from the analysis. Shield-ablated embryos were analysed by *in situ* hybridization for both *pitx2* [33] and for *sonic hedgehog* (*shh*) [98] transcripts. Only shield-ablated embryos that seemed to develop normally (see above), but yet had gaps of *shh* expression in the notochord and floorplate, were included in the analysis.

(d) *In situ* hybridization and microscopy

In situ hybridization was performed using standard techniques. Transplanted cells were detected with anti-fluorescein antibodies conjugated to HRP (Roche) and developed using DAB substrate and hydrogen peroxide. Plasmids used for *in situ*: *pitx2* [33] and *sonic hedgehog* (*shh*) [98]. Embryos were mounted in Permount® (Fisher) and photographed on a Zeiss Axioplan microscope equipped with a Zeiss AxioCam digital camera. Images were adjusted for brightness and contrast with Adobe Photoshop 5.5.

3. Results

(a) Abnormal expression of *pitx2* in LZ*oep* embryos

oep mutants in which the early requirement for *oep* is rescued by *oep* mRNA injection at the 1-cell stage—generating late-zygotic *oep* (LZ*oep*) mutants—develop L–R asymmetry defects. In these embryos, the asymmetric expression of *pitx2*, *spaw*, *cyclops* and *lefty2* is predominantly absent in the LPM and dorsal diencephalon of 18–22 somite LZ*oep* embryos ([33–35] and R.D.B., data not shown; figure 1). While wild-type levels of *pitx2* are never observed, further characterization reveals that a small percentage of LZ*oep* embryos express weak levels of *pitx2* in the LPM ($n = 33/246$; 13.5%; figure 1*c*,*d*,*e*). In these embryos, *pitx2* was found in small patches of cells within areas of the LPM where *pitx2* would normally be expressed. This expression was not restricted to a particular area along the anterior–posterior axis. Weak expression of *pitx2* was never observed in the dorsal diencephalon of LZ*oep* embryos (data not shown). The weak expression observed in LZ*oep* embryos was not restricted to the left LPM, but was also observed on the right ($n = 11/33$) or bilaterally in the left and right LPM ($n = 1/33$; figure 1*e*). These observations suggest that there are two defects in asymmetric gene expression in LZ*oep* embryos. First, *pitx2* expression is not induced to wild-type levels in the LPM. Second, in those embryos that do exhibit LPM *pitx2* expression, proper establishment of the asymmetric L–R pattern of *pitx2* does not occur.

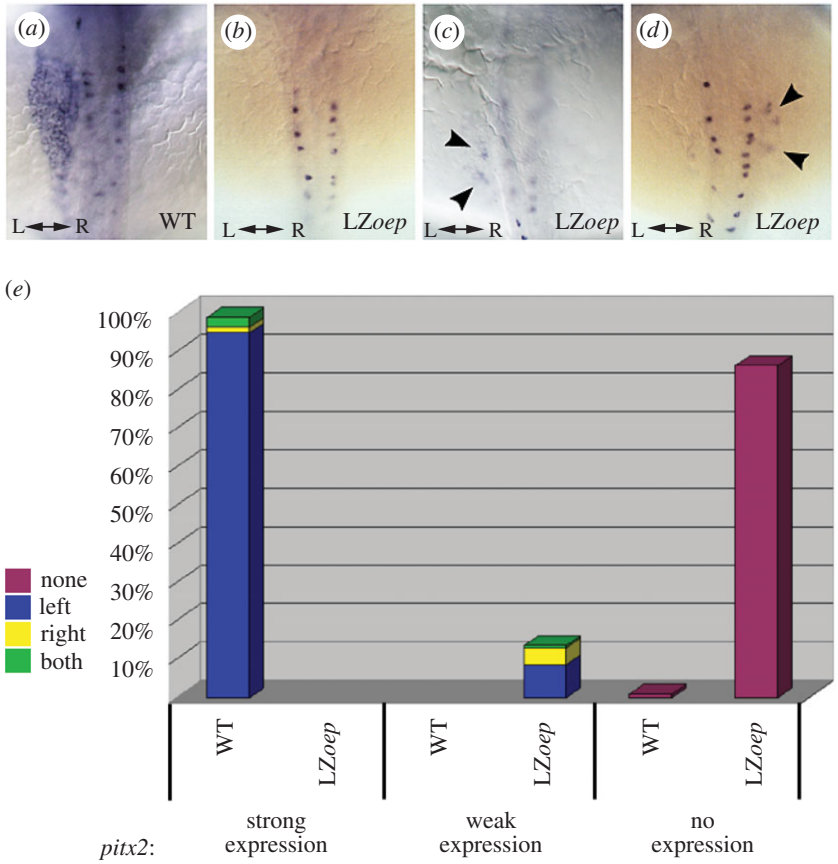

Figure 1. *pitx2* expression is abnormal in LZ*oep* embryos. Dorsal views of *pitx2* expression in wild-type (*a*) and LZ*oep* (*b–d*) embryos at the 18 somite stage. *pitx2* is expressed in presumed Rohon-Beard neurons in the spinal cord that form columns on either side of the midline. The LPM lies on both sides of the midline and normally expresses *pitx2* robustly on the left (*a*). In LZ*oep*, *pitx2* expression is either absent from the LPM (*b*) or is expressed in a few clumps of cells (arrowheads in *c*,*d*). Anterior is up; left (L) and right (R) are indicated. (*e*) Bar graph representing *pitx2* expression in wild-type ($n = 535$) and LZ*oep* ($n = 246$) embryos. In this and the following graphs, the percentage of embryos expressing *pitx2* is indicated by bars. Embryos were placed into one of three categories: strong expression (as in *a*), weak expression (as in *c*,*d*) or no expression (as in *b*). Each bar is colour coded to illustrate the sidedness of expression. Left LPM expression alone is marked in dark blue. Yellow denotes the population where expression was found only in the right LPM. Green denotes embryos where expression was found in both the left and right LPM. Non-expressing embryos are denoted by the maroon bar in the 'no expression' category. Both the strength of *pitx2* expression and the side of *pitx2* expression were significantly different between wild-type and LZ*oep* embryos ($p < 0.00001$ in both cases; χ^2-test applied).

(b) *oep* in the midline of LZ*oep* embryos can restore *pitx2* expression

The loss of *pitx2* LPM expression in LZ*oep* embryos is owing to insufficient *oep* activity. To determine the spatial requirement for *oep* in *pitx2* expression in the LPM, we generated genetic chimeras by transplantation. Asymmetric *pitx2* expression in the LPM is first observed at 10 somites in wild-type embryos (figure 2*f*) and is present through 26 h post fertilization (hpf). During somitogenesis, *oep* is expressed in the left and right LPM, in the developing dorsal diencephalon and in derivatives of axial mesoderm including the midline notochord, overlapping with *lefty1* expression ([31]; figure 2*d*,*g*). As Oep is required for Nodal signalling, and *pitx2* is a known target of Nodal signalling, it is conceivable that *oep* is predominantly required in the LPM to allow Nodal ligand to induce *pitx2* to be expressed at wild-type levels. To test this possibility, we first transplanted wild-type cells into 1000-cell stage LZ*oep* embryos. Transplantation at this early stage places wild-type cells in a scattered fashion throughout many tissues in the embryo. LZ*oep* embryos with wild-type cells in the LPM were obtained, but rescue of *pitx2* levels was not observed ($n = 10$). Large numbers of cells can be placed more accurately into the LPM by performing margin transplants at the 50% epiboly stage. Despite having large numbers of wild-type cells in the LPM, but not in other tissues, 10/14 showed no *pitx2* expression in the LPM and 4/14 showed weak expression of *pitx2* similar to LZ*oep* controls. This suggests that providing Oep in the LPM does not allow for Nodal signalling to occur in an embryo otherwise lacking Oep.

As *oep* is also expressed in the midline during the stages when *pitx2* is first expressed in the LPM (figure 2*d*,*g*), *oep* may be required in the midline to affect *pitx2* expression. We tested this hypothesis by placing wild-type cells into the midline of LZ*oep* embryos using shield transplantation (figure 3*a*) [96,97]. The zebrafish shield is equivalent to the organizer in *Xenopus* and gives rise to axial mesoderm and floor plate. In these experiments, the shield of the host embryos was removed and replaced by the shield from the donor. This type of transplantation places donor cells throughout the floor plate and axial mesoderm derivatives, including the hatching gland, head mesoderm and notochord (figure 3*b*). We did not observe transplanted cells in the dorsal forerunner cells or in KV with this procedure (data not shown). Transplantation of a wild-type shield into a wild-type host does not strongly affect the levels or the asymmetric expression of *pitx2* in the LPM (figure 3*c*,*e*,*f*), indicating that this form of transplantation does not robustly impact normal L–R patterning *per se*. While strong levels of *pitx2* were never observed in LZ*oep* controls, wild-type shields transplanted into LZ*oep* embryos were

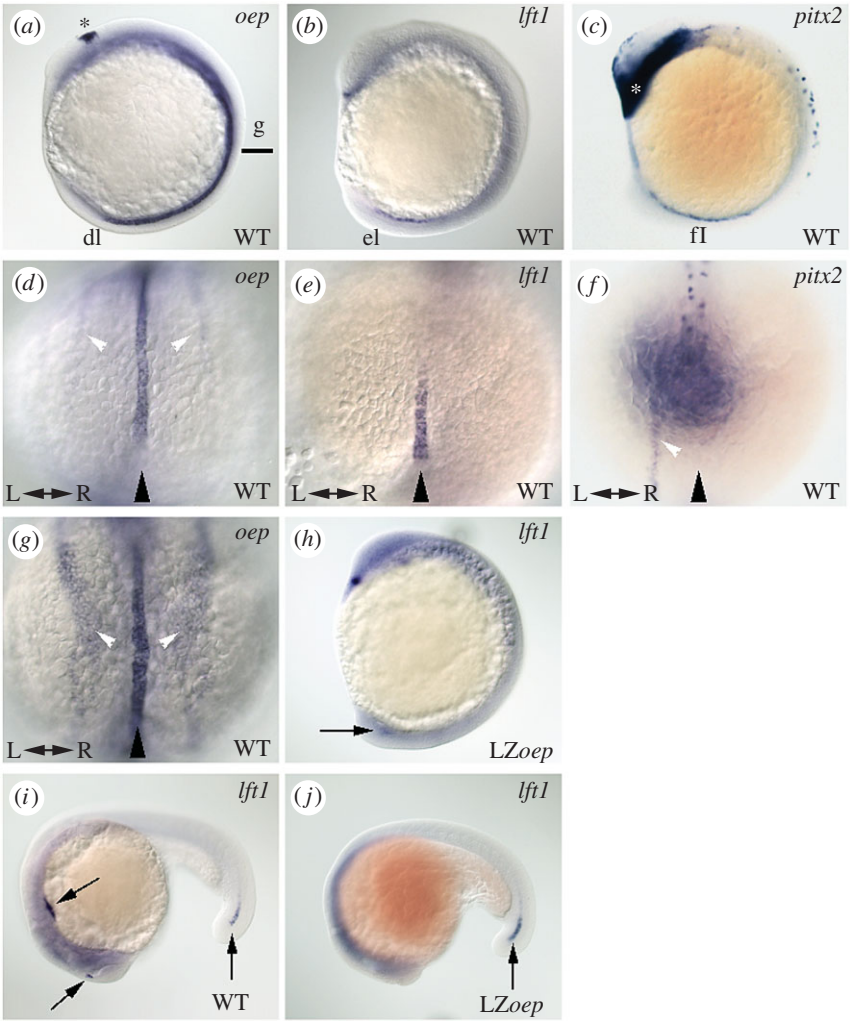

Figure 2. Expression of *one-eyed pinhead*, *lefty1* and *pitx2*. (*a*–*c*) Lateral views of wild-type embryos at the 10 somite stage. Anterior is up; dorsal to the right. Lines and lower case letters mark the level of the embryo shown in (*d*–*g*). (*d*–*f*) posterior views and (*g*) dorsal view of the embryos in (*a*–*c*). Anterior is up; left (L) and right (R) are indicated. *oep* is expressed in the dorsal diencephalon (asterisk in *a*), in the midline (black arrowhead in *d,g*) and in the LPM (white arrowheads *d,g*). At this stage, *oep* is expressed in thin stripes in the posterior LPM (*d*) and more broadly in more anterior parts of the LPM (*g*). *lft1* is expressed in a small portion of the anterior prechordal plate (dot of expression in the head region of *b*) and in the posterior midline (black arrowhead in *e*). The posterior notochord expression of *lft1* is observed even earlier at the 3 somite stage, prior to when the first asymmetric expression of *pitx2* is observed. *pitx2* is expressed in head mesoderm (asterisk in *c*) and in presumptive Rohon-Beard neurons in the spinal cord. The first asymmetric expression of *pitx2* is evident at this stage (white arrowhead in *f*) to the left of the midline (black arrowhead). Note the view in (*f*) is slightly displaced to those in (*d,e*) to better view the asymmetric expression of *pitx2*. The dark shading in (*f*) is from the expression in head mesoderm (asterisk in *a*) directly opposite the plane of view. (*h*) Expression of *lft1* in an LZ*oep* embryo at the 10 somite stage. *lft1* expression can vary from weak to undetectable (10/13; as shown in (*h*), indicated by black arrow), to almost wild-type in intensity (3/13). As *lft* is induced by Nodal, the loss of late Nodal signalling in LZ*oep* embryos may prevent the full induction of *lft1* observed in wild-type embryos. Accordingly, more embryos express *lft1* at the 3 somite stage (6/12 wild-type levels; 6/12 weaker levels). (*i*) Lateral view of *lft1* expression in an 18–20 somite stage wild-type embryo. Arrows mark expression domains in the diencephalon, the heart field and the posterior notochord [82,84]. (*j*) Lateral view of *lft1* expression in an LZ*oep* embryo at the 18–20 somite stage. Note only the expression domain in the posterior notochord (black arrow) is observed in LZ*oep* embryos (5/8 wild-type to reduced levels; 3/8 no obvious expression).

capable of restoring *pitx2* expression to strong levels, similar to wild-type, in the LPM in a proportion of embryos (figure 3*d*,*e*,*f*). To further ensure that this result is not simply a consequence of the transplantation technique, shields from LZ*oep* embryos were transplanted into LZ*oep* hosts. These transplanted embryos expressed weak levels of *pitx2* similar to LZ*oep* controls, but strong levels of expression were not observed (figure 3*e*). These results suggest that restoring *oep* expression in the midline can promote *pitx2* expression in the LPM in LZ*oep* embryos. Given that *pitx2* is a *bona fide* Nodal transcriptional target, and Nodal requires EGF-CFC proteins to function, we assume any *pitx2* expression in the LPM requires that residual Oep protein supplied via injection is still present.

To determine if a particular region of the midline must express *oep* to activate *pitx2* in the LPM, we monitored where transplanted cells were located. We did not find any correlation between the position of wild-type cells in the midline at the 18 somite stage and rescue of *pitx2* expression in the LPM of LZ*oep* embryos. For example, some LZ*oep* embryos with strong expression of *pitx2* had wild-type cells only in the most anterior floorplate cells, while others had wild-type cells throughout all axial mesoderm derivatives (data not shown). Intriguingly, while placing wild-type cells into the midline of LZ*oep* hosts could restore *pitx2* expression to strong levels in some cases, it did not correct the randomization of *pitx2* expression seen in LZ*oep* embryos (see §4).

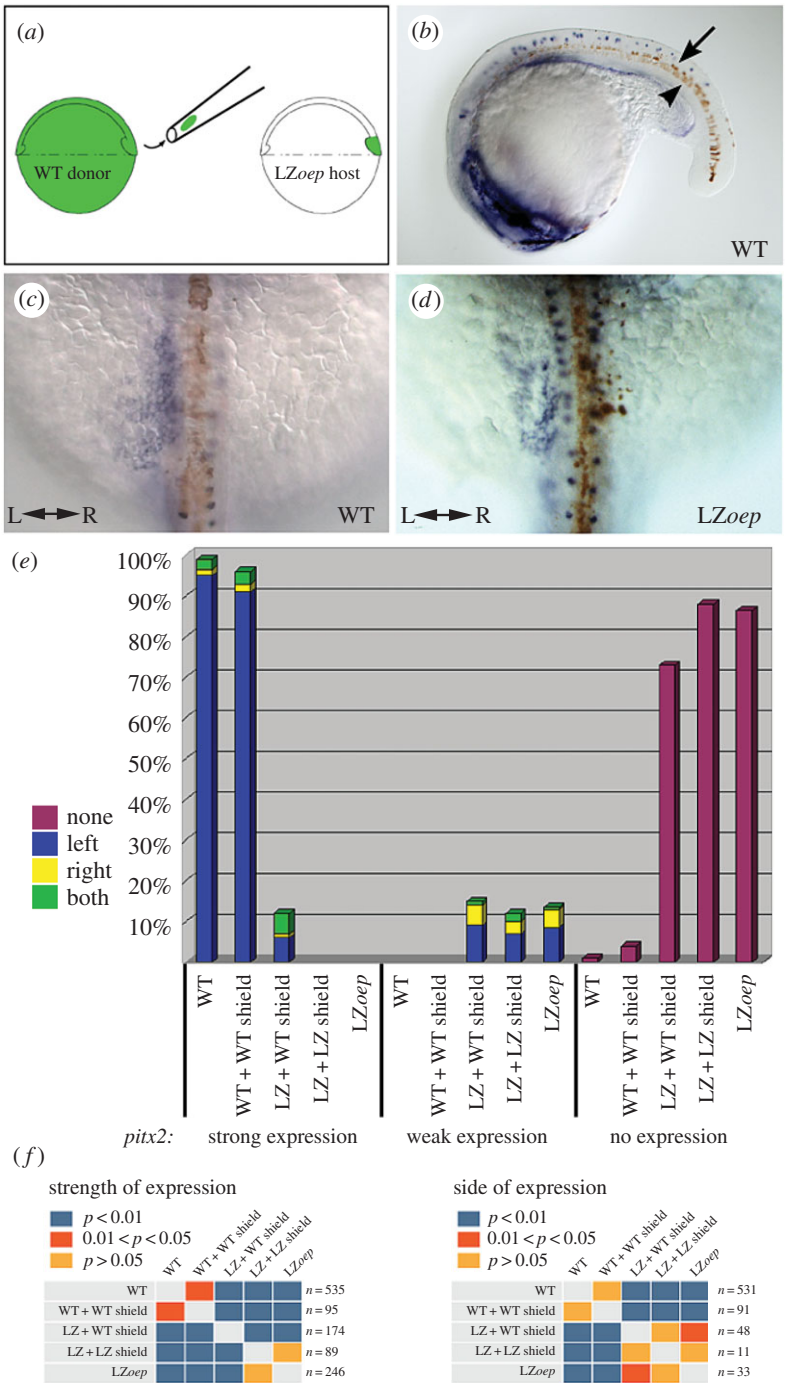

Figure 3. Shield transplantation experiments in wild-type and LZ*oep* embryos. (*a*) Illustration of the experiment. A needle is used to remove the shield from a donor embryo labelled with fluorescein dextran tracer dye. The shield from the host embryo is removed and replaced with the shield from the donor. (*b*) Lateral view of a wild-type embryo after a wild-type shield transplant. *pitx2* expression is in blue, labelled cells from the donor shield are in brown. Note that the floorplate (black arrow) and the notochord (black arrowhead) can be labelled with this technique. Labelled cells were not observed in the dorsal forerunner cells or in KV (data not shown). Dorsal views of *pitx2* expression in a wild-type embryo with a wild-type shield transplant (*c*) and an LZ*oep* embryo with a wild-type shield transplant (*d*) at the 18 somite stage. Anterior is up; left (L) and right (R) are indicated. (*e*) Bar graph representing *pitx2* expression in shield transplanted embryos. The genotype of the host is listed first, followed by the genotype of the donor. Expression categories and colour codes are described in figure 1. (*f*) Statistical significance of the experiments was determined using χ^2 and Fisher's exact tests. Comparisons of strength of *pitx2* expression and the sidedness of *pitx2* expression were conducted. For sidedness, only embryos that displayed expression were included in the analysis, reflected by the change in *n* values. Blue denotes *p*-values of less than 0.01, orange denotes *p*-values between 0.01 and 0.05, and light orange denotes *p*-values greater than 0.05.

(c) Blocking *ntla* activity in LZ*oep* embryos can restore *pitx2* expression

Our transplantation experiments suggest that the midline-localized *oep* has an active role in promoting *pitx2* expression in the LPM. This is in apparent contrast with models that support a more passive role for the midline (see §1). To further test the function of the midline in L–R patterning, we removed midline structures from LZ*oep* embryos using morpholino antisense oligonucleotides (MO) against *no tail* (*ntla*; the zebrafish *Brachyury/T* orthologue) [99]. *ntla* mutants and morphants lack the notochord, have expanded floorplate, have a substantially reduced KV and display bilateral expression of *pitx2* and other left side-specific genes [29,34,35,77,78,100–103]. Injection

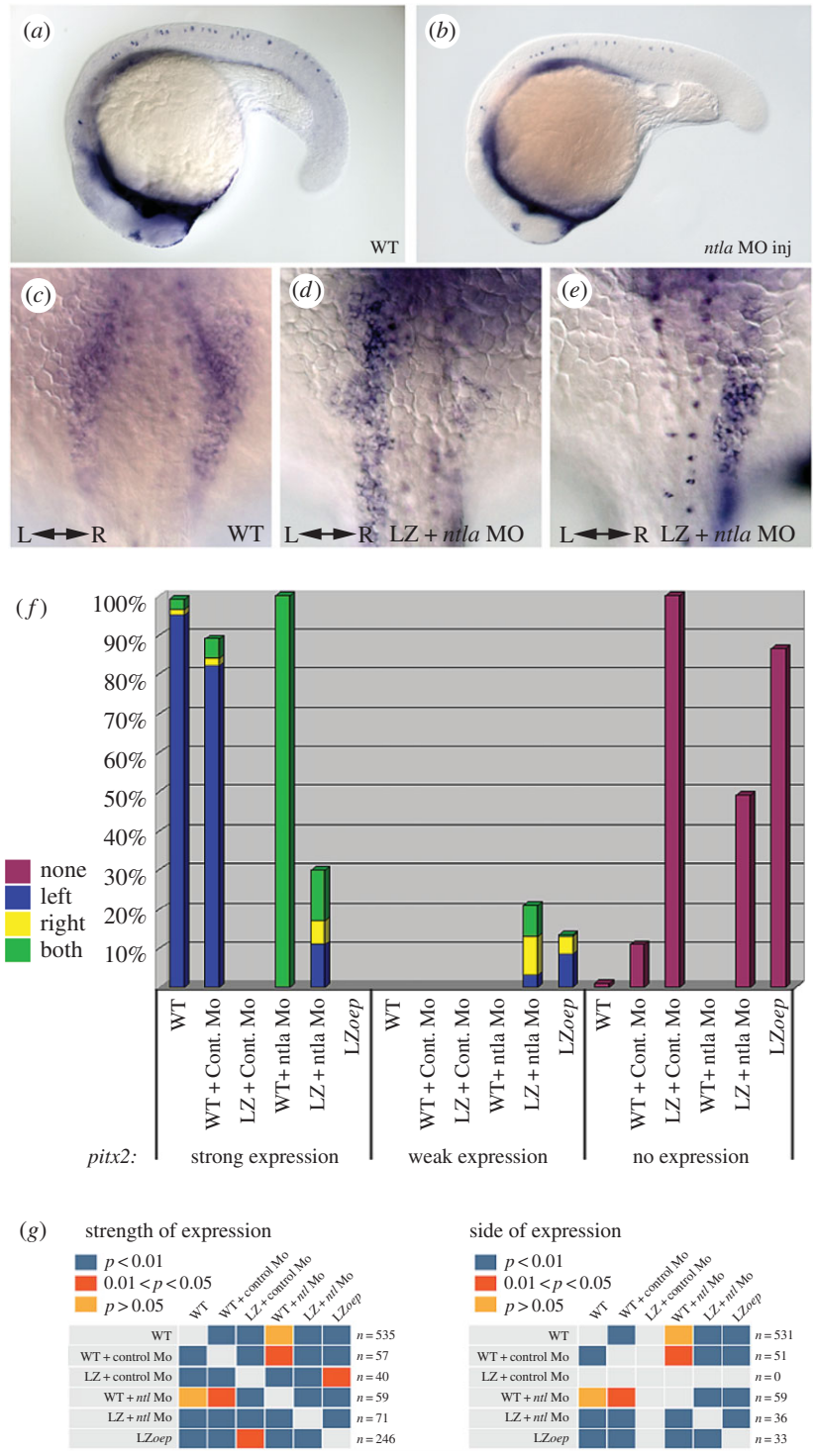

Figure 4. *no tail* (*ntla*) morpholino (MO) injections in wild-type and LZ*oep* embryos. Lateral views of 20 somite stage wild-type embryos injected with a control MO (*a*) or the *ntla* MO (*b*). Note the shortening of posterior structures in the *ntla* MO-injected embryo. Dorsal views of *pitx2* expression in *ntla* MO-injected wild-type (*c*) and LZ*oep* (*d,e*) embryos at the 18 somite stage. Anterior is up; left (L) and right (R) are indicated. (*f*) Bar graph representing *pitx2* expression in *ntla* MO-injected embryos. Genotype of injected embryos is listed first, followed by the injected MO. Expression categories and colour codes are described in figure 1. (*g*) Statistical significance of experiments conducted as described in figure 3.

of the *ntla* MO in wild-type or LZ*oep* embryos results in 100% of the injected embryos displaying the morphological *ntla* phenotype. In wild-type embryos injected with *ntla* MO, *pitx2* is expressed bilaterally as is seen in *ntla* mutants (figure 4*c*). Surprisingly, injection of *ntla* MO into LZ*oep* embryos can restore expression of *pitx2* in the LPM to strong levels in many cases; while LZ*oep* mutants never exhibited strong LPM *pitx2*, 30% of LZ*oep* mutants injected with *ntla* MO showed strong levels (figure 4*d–g*). Unlike injection of *ntla* MO, injection of a control MO does not dramatically alter *pitx2* gene expression levels in wild-type or LZ*oep* embryos (figure 4*f,g*). The most parsimonious explanation for these results is that the notochord and/or KV in LZ*oep* embryos represses *pitx2* transcription in the LPM, and that this repression can be released by blocking *ntla* function and removing midline structures.

(d) Midline ablations in LZ*oep* embryos can restore *pitx2* expression

Loss of *ntla* affects the notochord and the structure of KV [100,103]. To test if the phenotype of *ntla* MO-injected

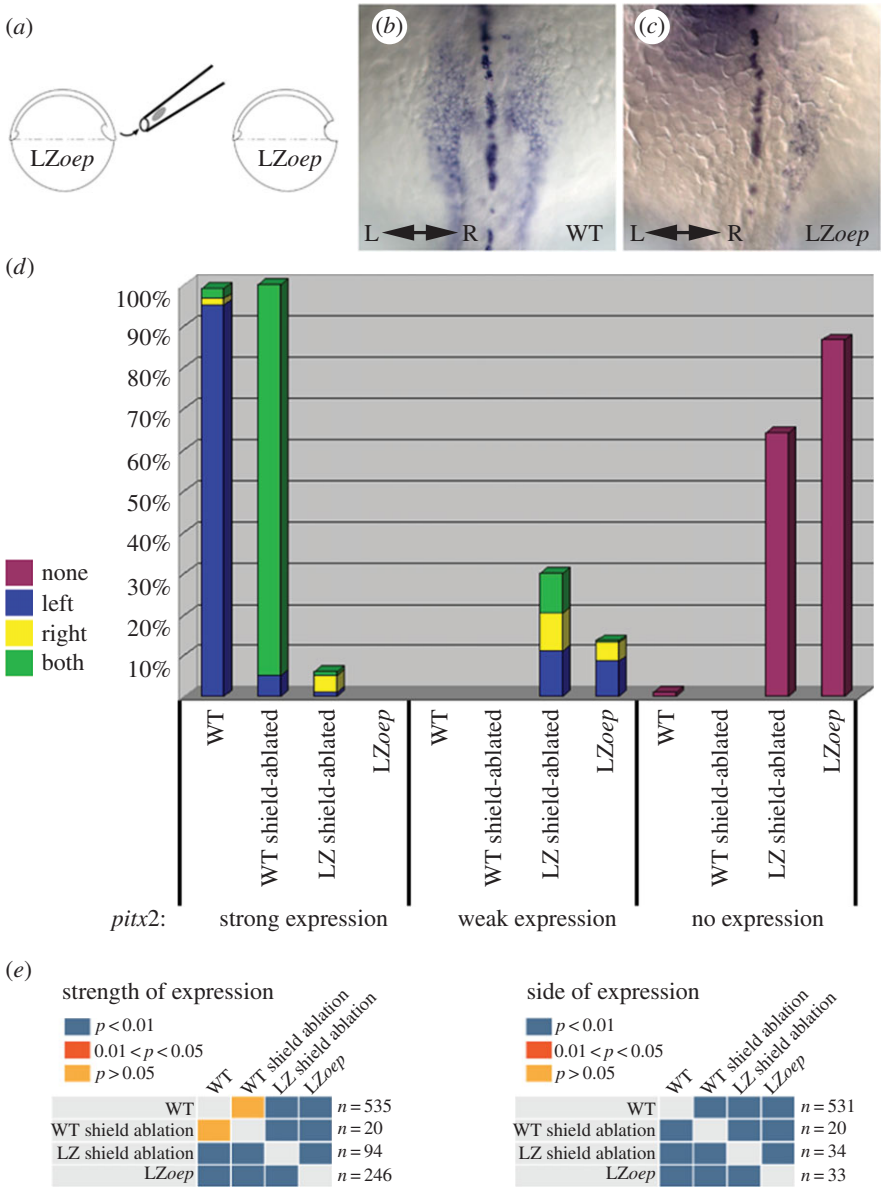

Figure 5. Shield ablations in wild-type and LZ*oep* embryos. (*a*) Illustration of shield ablation experiment. A needle is used to remove the shield, and cells on either side of the shield. Dorsal views of *pitx2* and *shh* expression in shield-ablated wild-type (*b*) and LZ*oep* (*c*) embryos at the 18 somite stage. Anterior is up; left (L) and right (R) are indicated. Damage to the midline in (*b*,*c*) is observed as gaps in the normally continuous *shh* expression in the midline. Note that these images are focused on the *shh* expression in the embryos, thus the *pitx2* expression in the Rohan-Beard neurons is not as visible. (*d*) Bar graph representing *pitx2* expression in shield-ablated embryos. Expression categories and colour codes are described in figure 1. (*e*) Statistical significance of experiments conducted as described in figure 3.

LZ*oep* embryos is owing to loss of the notochord specifically, we removed portions of the midline by shield ablation. Portions of the shield, and cells on either side of the shield, were removed by suction with a needle (figure 5*a*; [96]). The damaged shield region only partially regenerates, resulting in embryos that often have gaps in the notochord and floorplate as can be detected by *in situ* hybridization of the midline marker *sonic hedgehog* (*shh*). To select against embryos with non-axial mesoderm tissue losses, only embryos that appeared to develop normally, but had gaps in midline *shh* expression, were included in the analysis (see §2).

When shields were ablated in wild-type embryos, the majority of embryos expressed *pitx2* bilaterally in the LPM, indicating that damage to the midline affects *pitx2* expression as expected (figure 5*b*,*d*). Shield ablation in LZ*oep* embryos increased the number of embryos that weakly expressed *pitx2* and restored *pitx2* expression in the LPM to strong levels in some embryos, results that were statistically significantly different from non-ablated LZ*oep* embryos (figure 5*c*–*e*). Compared with *ntla* MO injection, the extent of midline removal is considerably less in shield-ablated LZ*oep* embryos and, accordingly, the proportion of LZ*oep* embryos expressing strong levels of *pitx2* was lower. Taken together, the effects of *ntla* MO and shield ablation in LZ*oep* embryos demonstrate that disruption of the notochord can restore LPM *pitx2* expression to strong levels in LZ*oep* embryos.

(e) Blocking *lefty1* activity in LZ*oep* embryos can restore *pitx2* expression

lefty1, the feedback inhibitor of Nodal, is expressed in the notochord of zebrafish embryos [82,84], and knockdown of *lefty1* results in bilateral expression of Nodal targets in the LPM [80,104]. We note that zebrafish *lefty1* (*lft1*) is expressed during early somitogenesis in the posterior midline, just anterior to KV, prior to the initiation of asymmetric gene expression in the LPM (this study and see [84]). At the

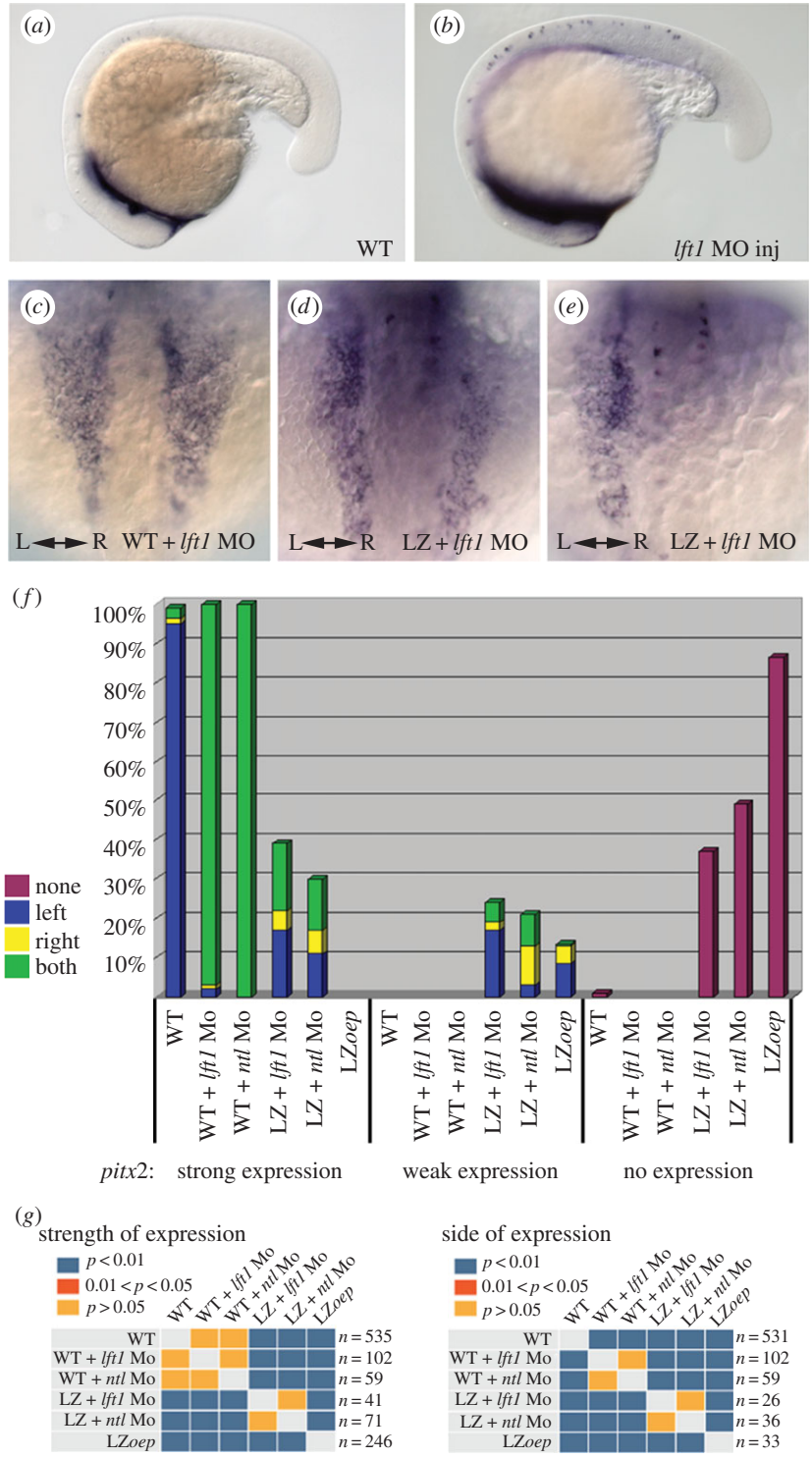

Figure 6. *lft1* MO injections in wild-type and LZ*oep* embryos. Lateral views of 18–20 somite stage LZ*oep* embryos injected with a control MO (*a*) or the *lft1* MO (*b*). *lft1*-injected embryos developed without apparent defects, but were often slightly delayed compared with uninjected controls. Dorsal views of *pitx2* expression in *lft1* MO-injected wild-type (*c*) or LZ*oep* (*d*,*e*) embryos at the 18 somite stage. Anterior is up; left (L) and right (R) are indicated. (*f*) Bar graph representing *pitx2* expression in MO-injected embryos. Genotype of injected embryos is listed first, followed by the injected MO. The *ntla* MO results from figure 4 are shown here to aid in comparison with the *lft1* MO results. Expression categories and colour codes are described in figure 1. (*g*) Statistical significance of experiments conducted as described in figure 3.

3 somite stage, 11/11 wild-type embryos expressed *lft1* in the posterior notochord region. Asymmetric *pitx2* expression begins at the 10 somite stage in the posterior LPM, just lateral to the *lft1* expression domain in the midline (figure 2*e*,*f*). We also detect *lft1* expression in the midline of LZ*oep* embryos at early and late somitogenesis stages, but sometimes at lower levels (figure 2*h*,*j*).

To test if *lft1* plays a role in the midline-dependent repression we observe, we injected MO against *lft1* into wild-type and LZ*oep* embryos. Injection of low levels of the *lft1* MO into wild-type embryos does not affect morphogenesis through somitogenesis (figure 6*a*,*b*; also see [80,104]), but results in predominantly bilateral expression of *pitx2* (figure 6*c*,*f*). This pattern of expression is statistically no different from that observed upon midline removal using the *ntla* MO (figure 6*f*,*g*). Indeed, injection of *lft1* MO into LZ*oep* embryos can restore *pitx2* expression to strong levels in the LPM, strikingly similar to what is observed when the midline is ablated in LZ*oep* embryos (figure 6*d*–*g*).

These results indicate that *lft1* is required for the repression of LPM *pitx2* expression in LZ*oep* mutants.

(f) *oep* in the midline of LZ*oep* embryos does not rescue randomization of *pitx2* expression

The results above show that the major phenotype of LZ*oep* embryos, the strong reduction of *pitx2* expression in the LPM, can be rescued by providing *oep* in the midline, ablating the midline or by blocking *lft1* function. To determine if the second phenotype in LZ*oep* mutants, the randomized induction of *pitx2*, is also rescued in these treatments, we monitored the L–R distribution of *pitx2* expression in all experiments. We find that manipulations that rescued *pitx2* expression to strong levels did not restore expression solely in the left LPM but also resulted in right LPM expression (figures 3*e*, 4*f* and 5*d*). Additionally, manipulations that resulted in bilateral *pitx2* expression in wild-type embryos did not consistently result in bilateral expression in LZ*oep*. For instance, knockdown of *ntla* results in bilateral *pitx2* expression in WT embryos but randomized expression in those LZ*oep* embryos that express any LPM *pitx2* (figure 4*f*). This suggests that there is an additional role for Oep in establishing or promoting asymmetric gene expression that is not rescued in our experiments.

4. Discussion

Since the first experiments that implicated the notochord in L–R patterning, the importance of an intact midline in this process has emerged from mutant analysis, gene knockdown experiments and midline extirpations. The results presented here suggest both an activating role and a repressive role for the midline in promoting transcription of *pitx2* in the LPM in zebrafish. In LZ*oep* embryos, the loss of strong *pitx2* expression levels in the LPM can be rescued by introducing wild-type cells into the midline. This suggests that *oep* in the midline can actively promote *pitx2* expression in the LPM. Furthermore, we show that removal of midline structures from LZ*oep* embryos, either by shield ablations or injection of *ntla* MO, can also restore *pitx2* expression to strong levels in the LPM. This suggests that the midline represses *pitx2* in the LPM. These results can be reconciled by a model in which *oep* in the midline functions to overcome a midline-derived repressor of LPM Nodal activity.

(a) A model for Lefty and Oep function prior to asymmetric gene expression during the establishment of L–R asymmetry: the midline as an 'activator' and 'repressor'

Based on our results, and previously proposed models for the establishment of L–R asymmetry, we propose the following model for L–R patterning in zebrafish (figure 7*a–c*). Both the left and right LPM have the potential to express left side-specific genes such as *pitx2*, which typically occurs at the 10 somite stage. *lft1* expression (dark blue; figure 7*a*) is induced in the posterior notochord prior to 10 somites, most likely by an earlier Nodal signalling event. Indeed, at the 3 somite stage, robust *lft1* can be observed in this domain. Lefty1 from this midline domain increases the amount of Nodal ligand required to induce LPM-*nodal* (i.e. raises the threshold required for robust Nodal activation) and thus represses *pitx2* transcription (black inhibition arrows; figure 7*a*). This occurs symmetrically and prevents LPM Nodal activation prematurely, before the symmetry-breaking event at KV has occurred. An *oep*-dependent process in the midline weakens repression by Lefty1 (grey inhibition arrows; figure 7*b*). As Lefty can bind to Oep, and overexpression of Oep can suppress the effects of overexpressing Lefty [8], we suggest that physical interaction between Lefty1 and Oep at the midline sequesters some Lefty1, thereby reducing the effective amount of Lefty1 able to repress LPM Nodal signals. This antagonism of Lefty1 by Oep would thus allow Nodal signals to activate transcription in the LPM (light purple; figure 7*b*).

While the early interaction between *oep* and *lft1* that our experiments have uncovered is important for allowing Nodal signals to initiate in the LPM, it may be less critical for setting up the asymmetry of these signals. After all, the early domain of *lft1* is L–R symmetrical and we would expect this to dampen Nodal signalling in both the left and right LPM equally. Instead, asymmetries in LPM Nodal activity are generated downstream of asymmetric flow in KV and the resulting left-sided downregulation of the Nodal repressor *charon*. Flow-dependent downregulation of *charon* and *oep*-dependent dampening of Lefty in the midline would thus cooperate to generate a signalling threshold in which Nodal signals are able to robustly activate in the left LPM around the 10 somite stage but not in the right LPM. Subsequently, Nodal signals spread anteriorly in the left LPM and induce further *lft1* expression in the notochord (figure 7*c*), which then acts to maintain asymmetry by preventing Nodal signals from activating and spreading in the right LPM.

This model can explain the phenotypes we observe in LZ*oep* embryos as well as in the various treatments (ablations, transplants and MO injections) performed in this study. In LZ*oep* embryos (figure 7*d–g*), *lft1* is still present in the posterior notochord (figure 7*d*). This expression of *lft1* is likely owing to residual Oep protein from the 1-cell *oep* mRNA injection at the time when *lft1* is induced, several hours before *pitx2* is initiated in the LPM. However, in these same embryos, later *oep* function is greatly reduced. This late reduction in Oep in LZ*oep* mutants, therefore, results in more active Lefty repressor in the posterior notochord; thus, Nodal signals are repressed at a level that prevents them from initiating target gene expression in the LPM (figure 7*e*). Removing the repressor by loss of the midline (*ntla* MO (figure 7*g*) or shield ablation) or by reducing *lft1* itself (figure 7*f*) is sufficient to allow for signalling to occur in the LPM of LZ*oep* mutants because these treatments replace the requirement of Oep to repress Lefty. Importantly, these treatments also suggest that there is sufficient functioning Oep in the LPM of LZ*oep* embryos to allow for robust Nodal activity; thus, the lost or weakened *pitx2* expression in LZ*oep* is not exclusively a consequence of loss of Oep in the LPM. This agrees with our finding that adding Oep-positive cells to the LPM of LZ*oep* mutants cannot rescue high levels of LPM *pitx2* expression. Furthermore, although the potential for rescue is clear, we suggest that the rescue of LPM *pitx2* in LZ*oep* mutants, either after wild-type shield transplants or injection of *ntla* MO, is only partial because the LPM still has limited functional Oep remaining from the early mRNA *oep* injection.

This model is consistent with the timing and location of *lft1*, *pitx2* and *oep* expression. Zebrafish *lft1* is expressed in

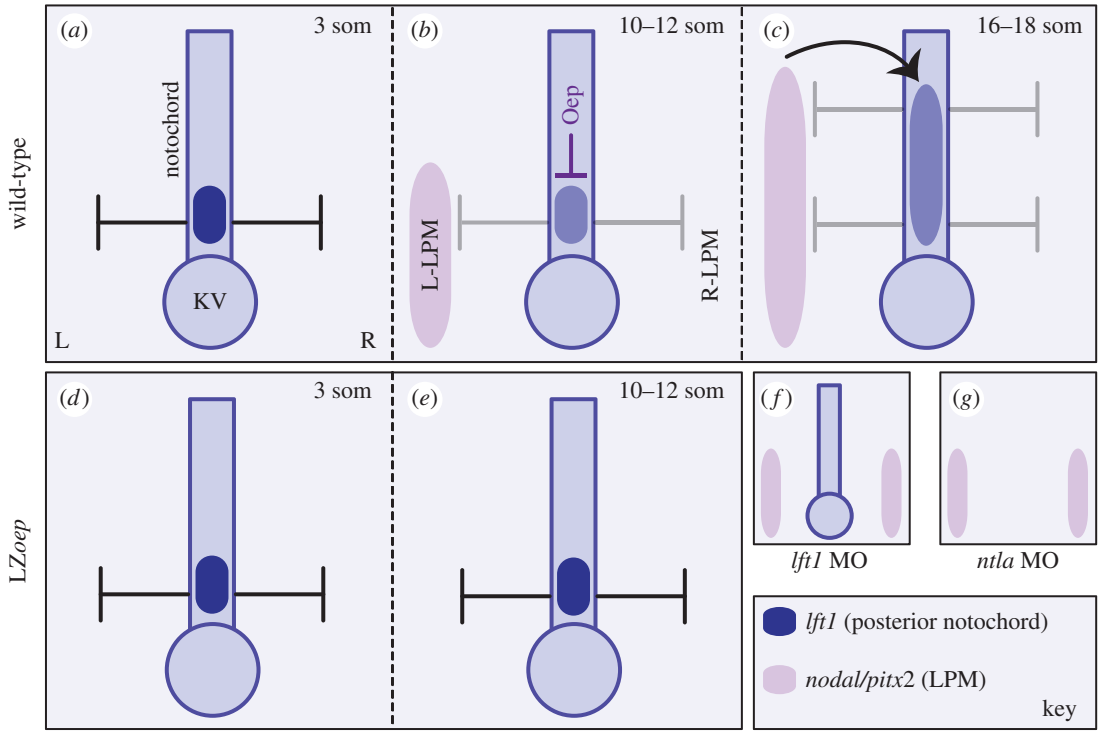

Figure 7. Model depicting antagonism of Lefty by Oep prior to the emergence of asymmetric gene expression in the zebrafish LPM. All renderings are of the notochord and surrounding LPM. The notochord terminates into KV (oval). (*a*) *lft1* is expressed in the posterior notochord before asymmetric gene expression is detected (dark blue). We postulate that Lefty acts to repress Nodal signalling to the LPM (black repression arrows) and thus prevents activation of Nodal target genes in the LPM prior to the L–R biasing event that occurs at KV. (*b*) An *oep*-dependent signalling event overcomes/weakens the midline repressor, Lefty (weaker repression depicted by grey repression arrows). This weakened repressor can still prevent Nodal activity from occurring in the LPM initially. A biasing mechanism, flow generated by monocilia in KV, leads to downregulation of the Nodal inhibitor *charon* around KV (not depicted) and allows Nodal signalling to initiate in the left LPM at around the 10 somite stage (light purple). (*c*) Nodal autoregulation then leads to the robust expression of left side-specific genes including *pitx2*. Nodal signalling to the right LPM continues to be repressed by the higher level of Charon on the right of KV in cooperation with Lefty from the midline. (*d*) In LZ*oep* embryos, the early posterior notochord *lft1* repressor is active and not weakened owing to the later absence of Oep. (*e*) Nodal signalling does not reach the threshold to overcome the repressors and robust transcription in the LPM does not take place. (*f*) In *lft1* MO-injected LZ*oep* embryos, the early posterior notochord repressor is removed, thus the threshold for Nodal to signal to the left and the right LPM is lower, and both sides can initiate transcription of left side-specific genes. (*g*) In *ntla* MO-injected LZ*oep* embryos, midline structures are absent and thus, there is no midline repressor. Nodal signalling can thus initiate transcription of left side-specific genes bilaterally even in LZ*oep* embryos as Oep is not required to overcome the repressor.

the posterior notochord preceding *pitx2* and *spaw* expression in the LPM. *pitx2* expression is observed later (beginning around the 10 somite stage) in the posterior-most LPM, just lateral to the posterior notochord and KV (figure 2). *lft1* expression in the midline later extends from the posterior notochord to the anterior, induced by Nodal from the LPM [87,88]. Our findings provide a previously unappreciated role for early *lft1* in establishing LPM Nodal signals.

Moreover, the model explains the results of our midline ablation experiments in wild-type and LZ*oep* embryos. Midline ablations result in bilateral expression of *pitx2* in wild-type embryos and can restore *pitx2* to strong levels in LZ*oep* mutants. In our model, the source of the repressor (the early domain of *lft1*), the notochord, is removed in these experiments, allowing Nodal signals to activate *pitx2* in the LPM strongly and bilaterally. It is worth noting that the biasing mechanism occurring at KV should be unaffected by these treatments as our transplants did not contribute to the dorsal forerunner or KV populations. Nevertheless, we likely see bilateral *pitx2* expression because loss of the early *lft1* repressor allows Nodal activity at both the left and right LPM to induce Nodal targets, regardless of subtle differences in Nodal levels caused by the biasing mechanism at KV. However, it is worth noting that KV function may not strictly be required for Nodal signalling in the LPM. In *ntla* mutants or embryos injected with *ntla* MO, ciliated cells are present, but KV does not form. Moreover, *spaw* expression around KV is lost in *ntla* mutants, suggesting that the activating signal for Nodal in the LPM in this mutant must come from another source that remains elusive at this point. It is possible that this LPM-*spaw* activation in the absence of KV-*spaw* occurs because *lft1* and *charon*, which both encode Spaw repressors, are also not expressed in *ntla* mutants, and therefore, the threshold for LPM-*spaw* activation is likely markedly reduced. Nevertheless, as KV-*spaw* is absent in *ntla* mutants, this observation calls into question the current major model that LRC Nodal signals induce the LPM Nodal cascade. In the mouse, node-derived Nodal is thought travel to the LPM and initiate *Nodal* expression there; indeed, *Nodal* mutants fail to activate LPM *Nodal* expression [24]. However, it is yet to be determined whether node-derived Nodal protein alone is sufficient to induce LPM *Nodal* in the endogenous context or whether node-Nodal is able to active the LPM Nodal cascade in the absence of inhibitors like *Cerl-2*. It is worth noting that, unlike what we report in zebrafish, it is thought that LPM Nodal signals are responsible for inducing floor-plate expression of *Lefty1* [85], and therefore, removing *Lefty1* from *Nodal* mutants would likely have no impact on whether the Nodal cascade is activated in the LPM.

(b) The role of midline Oep in generating the asymmetry of LPM Nodal signals

In addition to the role *oep* plays in promoting gene transcription in the LPM, our results also suggest another role for *oep* in establishing proper L–R pattern. The weak expression seen in some LZ*oep* embryos is not restricted to the left side, suggesting that the loss of *oep* leads to a randomization of the L–R pattern. We do not know where *oep* is required in this process, as *oep* in the midline did not rescue randomization in LZ*oep* mutants. As a result, this is more difficult to reconcile, but may be a consequence of the unique background that LZ*oep* embryos provide. The ability for Nodal to signal is likely waning during somitogenesis as Oep provided by RNA injection diminishes. LZ*oep* embryos with weak *pitx2* expression, and the fraction of embryos that respond with strong *pitx2* expression in our experiments, may encompass those with more residual Oep. Thus, it is possible that one-sided expression, versus bilateral, occurs in our experiments where the midline is removed in LZ*oep* embryos, owing to the amount of Oep available in the LPM for the response. Furthermore, L–R patterning can be easily disrupted by situations that alter the timing and expression of repressors and activators. In LZ*oep* embryos without additional treatments, the randomization of *pitx2* expression could likewise be owing to the indeterminate levels of Oep present, which may alter the timing of response to signals from the LRC.

As a final note, in addition to the midline, *oep* is also expressed in the LPM and diencephalon. The shield transplantations and midline ablations reported here did not restore *pitx2* expression in the diencephalon of LZ*oep* mutants (data not shown), suggesting that *oep* might be required in the diencephalon for expression to occur. We have previously shown that repression of left side-specific genes also occurs in the diencephalon [34], thus it is intriguing to speculate that *oep* also plays a role in overcoming this repression.

In summary, the results in this paper support a model wherein midline Oep functions to repress *lft1*, expressed in the notochord, thereby lowering the threshold and thus promoting activation of the Nodal cascade in the LPM.

Ethics. This work was conducted at the Skirball Institute of Biomolecular Medicine at New York University Langone Medical Center. Established zebrafish protocols were approved and adhered to in accordance with the Institutional Animal Care and Use Committee of New York University Langone Medical Center.

Data accessibility. The datasets supporting this article have been uploaded as part of the electronic supplementary material.

Authors' contributions. R.D.B. performed the experiments. R.D.B. and D.T.G interpreted the data, wrote and revised the manuscript, and approved of the final submission.

Competing interests. We have no competing interests

Funding. R.D.B. was supported in her postdoctoral position by a Damon Runyon Fellowship DRG-1491 from the Damon Runyon Cancer Research Foundation and by a postdoctoral fellowship from the American Heart Association Heritage Affiliate. Left–right patterning work in her laboratory is currently supported by a National Institute of Child Health and Development grant 2R01HD048584. D.T.G. is supported by a postdoctoral fellowship from the American Heart Association Founders Affiliate.

Acknowledgements. This work was conducted when R.D.B. was a postdoctoral fellow in the laboratory of Alexander F. Schier, and I thank Alex for his mentorship and support. I thank members of the Schier and Yelon laboratories for discussions; Derek Stemple for teaching me the shield transplantation procedure; and S. Zimmerman, T. Bruno and N. Dillon for fish care.

References

1. Burdine RD, Schier AF. 2000 Conserved and divergent mechanisms in left–right axis formation. *Genes Dev*. **14**, 763–776.
2. Levin M. 2005 Left–right asymmetry in embryonic development: a comprehensive review. *Mech. Dev*. **122**, 3–25. (doi:10.1016/j.mod.2004.08.006)
3. Nakamura T, Hamada H. 2012 Left–right patterning: conserved and divergent mechanisms. *Development* **139**, 3257–3262. (doi:10.1242/dev.061606)
4. Ramsdell AF. 2005 Left–right asymmetry and congenital cardiac defects: getting to the heart of the matter in vertebrate left–right axis determination. *Dev. Biol*. **288**, 1–20. (doi:10.1016/j.ydbio.2005.07.038)
5. Shiratori H, Hamada H. 2014 TGFβ signaling in establishing left–right asymmetry. *Semin. Cell Dev. Biol*. **32**, 80–84. (doi:10.1016/j.semcdb.2014.03.029)
6. Sampath K, Robertson EJ. 2016 Keeping a lid on nodal: transcriptional and translational repression of nodal signalling. *Open Biol*. **6**, 150200. (doi:10.1098/rsob.150200)
7. Schier AF. 2009 Nodal morphogens. *Cold Spring Harb. Perspect. Biol*. **1**, a003459. (doi:10.1101/cshperspect.a003459)
8. Cheng SK, Olale F, Brivanlou AH, Schier AF. 2004 Lefty blocks a subset of TGFβ signals by antagonizing EGF-CFC coreceptors. *PLoS Biol*. **2**, E30. (doi:10.1371/journal.pbio.0020030)
9. Gritsman K, Zhang J, Cheng S, Heckscher E, Talbot WS, Schier AF. 1999 The EGF-CFC protein one-eyed pinhead is essential for nodal signaling. *Cell*. **97**, 121–132. (doi:10.1016/S0092-8674(00)80720-5)
10. Reissmann E *et al*. 2001 The orphan receptor ALK7 and the Activin receptor ALK4 mediate signaling by Nodal proteins during vertebrate development. *Genes Dev*. **15**, 2010–2022. (doi:10.1101/gad.201801)
11. Yeo C, Whitman M. 2001 Nodal signals to Smads through Cripto-dependent and Cripto-independent mechanisms. *Mol. Cell*. **7**, 949–957. (doi:10.1016/S1097-2765(01)00249-0)
12. Hoodless PA *et al*. 2001 *FoxH1* (*Fast*) functions to specify the anterior primitive streak in the mouse. *Genes Dev*. **15**, 1257–1271. (doi:10.1101/gad.881501)
13. Slagle CE, Aoki T, Burdine RD. 2011 Nodal-dependent mesendoderm specification requires the combinatorial activities of FoxH1 and Eomesodermin. *PLoS Genet*. **7**, e1002072. (doi:10.1371/journal.pgen.1002072)
14. Yeo CY, Chen X, Whitman M. 1999 The role of FAST-1 and Smads in transcriptional regulation by activin during early *Xenopus* embryogenesis. *J. Biol. Chem*. **274**, 26 584–26 590. (doi:10.1074/jbc.274.37.26584)
15. Yoon SJ, Wills AE, Chuong E, Gupta R, Baker JC. 2011 HEB and E2A function as SMAD/FOXH1 cofactors. *Genes Dev*. **25**, 1654–1661. (doi:10.1101/gad.16800511)
16. Zhou S, Zawel L, Lengauer C, Kinzler KW, Vogelstein B. 1998 Characterization of human *FAST-1*, a TGFβ and activin signal transducer. *Mol. Cell*. **2**, 121–127. (doi:10.1016/S1097-2765(00)80120-3)
17. Pogoda HM, Solnica-Krezel L, Driever W, Meyer D. 2000 The zebrafish forkhead transcription factor FoxH1/Fast1 is a modulator of nodal signaling required for organizer formation. *Curr. Biol*. **10**, 1041–1049. (doi:10.1016/S0960-9822(00)00669-2)
18. Sirotkin HI, Gates MA, Kelly PD, Schier AF, Talbot WS. 2000 *fast1* is required for the development of dorsal axial structures in zebrafish. *Curr. Biol*. **10**, 1051–1054. (doi:10.1016/S0960-9822(00)00679-5)
19. Nonaka S, Tanaka Y, Okada Y, Takeda S, Harada A, Kanai Y, Kido M, Hirokawa N. 1998 Randomization of left–right asymmetry due to loss of nodal cilia generating leftward flow of extraembryonic fluid in mice lacking KIF3B motor protein. *Cell* **95**, 829–837. (doi:10.1016/S0092-8674(00)81705-5)

20. Schweickert A, Weber T, Beyer T, Vick P, Bogusch S, Feistel K, Blum M. 2007 Cilia-driven leftward flow determines laterality in *Xenopus*. *Curr. Biol*. **17**, 60–66. (doi:10.1016/j.cub.2006.10.067)
21. Essner JJ, Amack JD, Nyholm MK, Harris EB, Yost HJ. 2005 Kupffer's vesicle is a ciliated organ of asymmetry in the zebrafish embryo that initiates left–right development of the brain, heart and gut. *Development* **132**, 1247–1260. (doi:10.1242/dev.01663)
22. Essner JJ, Vogan KJ, Wagner MK, Tabin CJ, Yost HJ, Brueckner M. 2002 Conserved function for embryonic nodal cilia. *Nature* **418**, 37–38. (doi:10.1038/418037a)
23. Okada Y, Takeda S, Tanaka Y, Belmonte JC, Hirokawa N. 2005 Mechanism of nodal flow: a conserved symmetry breaking event in left–right axis determination. *Cell* **121**, 633–644. (doi:10.1016/j.cell.2005.04.008)
24. Brennan J, Norris DP, Robertson EJ. 2002 Nodal activity in the node governs left–right asymmetry. *Genes Dev*. **16**, 2339–2344. (doi:10.1101/gad.1016202)
25. Norris DP, Brennan J, Bikoff EK, Robertson EJ. 2002 The Foxh1-dependent autoregulatory enhancer controls the level of Nodal signals in the mouse embryo. *Development* **129**, 3455–3468.
26. Lowe LA, Yamada S, Kuehn MR. 2001 Genetic dissection of nodal function in patterning the mouse embryo. *Development* **128**, 1831–1843.
27. Oki S, Hashimoto R, Okui Y, Shen MM, Mekada E, Otani H, Saijoh Y, Hamada H. 2007 Sulfated glycosaminoglycans are necessary for Nodal signal transmission from the node to the left lateral plate in the mouse embryo. *Development* **134**, 3893–3904. (doi:10.1242/dev.009464)
28. Kawasumi A, Nakamura T, Iwai N, Yashiro K, Saijoh Y, Belo JA, Shiratori H, Hamada H. 2011 Left–right asymmetry in the level of active Nodal protein produced in the node is translated into left–right asymmetry in the lateral plate of mouse embryos. *Dev. Biol*. **353**, 321–330. (doi:10.1016/j.ydbio.2011.03.009)
29. Long S, Ahmad N, Rebagliati M. 2003 The zebrafish *nodal*-related gene *southpaw* is required for visceral and diencephalic left–right asymmetry. *Development* **130**, 2303–2316. (doi:10.1242/dev.00436)
30. Shen MM, Wang H, Leder P. 1997 A differential display strategy identifies Cryptic, a novel EGF-related gene expressed in the axial and lateral mesoderm during mouse gastrulation. *Development* **124**, 429–442.
31. Zhang J, Talbot WS, Schier AF. 1998 Positional cloning identifies zebrafish *one-eyed pinhead* as a permissive EGF-related ligand required during gastrulation. *Cell* **92**, 241–251. (doi:10.1016/S0092-8674(00)80918-6)
32. Gaio U *et al.* 1999 A role of the *cryptic* gene in the correct establishment of the left–right axis. *Curr. Biol*. **9**, 1339–1342. (doi:10.1016/S0960-9822(00)80059-7)
33. Yan YT, Gritsman K, Ding J, Burdine RD, Corrales JD, Price SM, Talbot WS, Schier AF, Shen MM. 1999 Conserved requirement for *EGF-CFC* genes in vertebrate left–right axis formation. *Genes Dev*. **13**, 2527–2537. (doi:10.1101/gad.13.19.2527)
34. Concha ML, Burdine RD, Russell C, Schier AF, Wilson SW. 2000 A Nodal signaling pathway regulates the laterality of neuroanatomical asymmetries in the zebrafish forebrain. *Neuron* **28**, 399–409. (doi:10.1016/S0896-6273(00)00120-3)
35. Liang JO *et al.* 2000 Asymmetric nodal signaling in the zebrafish diencephalon positions the pineal organ. *Development* **127**, 5101–5112.
36. Bamford RN *et al.* 2000 Loss-of-function mutations in the EGF-CFC gene *CFC1* are associated with human left–right laterality defects. *Nat. Genet*. **26**, 365–369. (doi:10.1038/81695)
37. Marjoram L, Wright C. 2011 Rapid differential transport of Nodal and Lefty on sulfated proteoglycan-rich extracellular matrix regulates left–right asymmetry in *Xenopus*. *Development* **138**, 475–485. (doi:10.1242/dev.056010)
38. Francescatto L, Rothschild SC, Myers AL, Tombes RM. 2010 The activation of membrane targeted CaMK-II in the zebrafish Kupffer's vesicle is required for left–right asymmetry. *Development* **137**, 2753–2762. (doi:10.1242/dev.049627)
39. McGrath J, Somlo S, Makova S, Tian X, Brueckner M. 2003 Two populations of node monocilia initiate left–right asymmetry in the mouse. *Cell* **114**, 61–73. (doi:10.1016/S0092-8674(03)00511-7)
40. Yuan S, Zhao L, Brueckner M, Sun Z. 2015 Intraciliary calcium oscillations initiate vertebrate left–right asymmetry. *Curr. Biol*. **25**, 556–567. (doi:10.1016/j.cub.2014.12.051)
41. Viotti M, Niu L, Shi SH, Hadjantonakis AK. 2012 Role of the gut endoderm in relaying left–right patterning in mice. *PLoS Biol*. **10**, e1001276. (doi:10.1371/journal.pbio.1001276)
42. Saund RS, Kanai-Azuma M, Kanai Y, Kim I, Lucero MT, Saijoh Y. 2012 Gut endoderm is involved in the transfer of left–right asymmetry from the node to the lateral plate mesoderm in the mouse embryo. *Development* **139**, 2426–2435. (doi:10.1242/dev.079921)
43. Beyer T, Thumberger T, Schweickert A, Blum M. 2012 *Connexin26*-mediated transfer of laterality cues in *Xenopus*. *Biol. Open*. **1**, 473–481. (doi:10.1242/bio.2012760)
44. Norris DP. 2012 Cilia, calcium and the basis of left–right asymmetry. *BMC Biol*. **10**, 102. (doi:10.1186/1741-7007-10-102)
45. Supatto W, Fraser SE, Vermot J. 2008 An all-optical approach for probing microscopic flows in living embryos. *Biophys. J*. **95**, L29–L31. (doi:10.1529/biophysj.108.137786)
46. Amack JD, Wang X, Yost HJ. 2007 Two T-box genes play independent and cooperative roles to regulate morphogenesis of ciliated Kupffer's vesicle in zebrafish. *Dev. Biol*. **310**, 196–210. (doi:10.1016/j.ydbio.2007.05.039)
47. Kreiling JA, Williams G, Creton R. 2007 Analysis of Kupffer's vesicle in zebrafish embryos using a cave automated virtual environment. *Dev. Dyn*. **236**, 1963–1969. (doi:10.1002/dvdy.21191)
48. Nonaka S, Shiratori H, Saijoh Y, Hamada H. 2002 Determination of left–right patterning of the mouse embryo by artificial nodal flow. *Nature* **418**, 96–99. (doi:10.1038/nature00849)
49. Nonaka S, Yoshiba S, Watanabe D, Ikeuchi S, Goto T, Marshall WF, Hamada H, Stemple D. 2005 De novo formation of left–right asymmetry by posterior tilt of nodal cilia. *PLoS Biol*. **3**, e268. (doi:10.1371/journal.pbio.0030268)
50. Kramer-Zucker AG, Olale F, Haycraft CJ, Yoder BK, Schier AF, Drummond IA. 2005 Cilia-driven fluid flow in the zebrafish pronephros, brain and Kupffer's vesicle is required for normal organogenesis. *Development* **132**, 1907–1921. (doi:10.1242/dev.01772)
51. Okabe N, Xu B, Burdine RD. 2008 Fluid dynamics in zebrafish Kupffer's vesicle. *Dev. Dyn*. **237**, 3602–3612. (doi:10.1002/dvdy.21730)
52. Borovina A, Superina S, Voskas D, Ciruna B. 2010 Vangl2 directs the posterior tilting and asymmetric localization of motile primary cilia. *Nat. Cell Biol*. **12**, 407–412. (doi:10.1038/ncb2042)
53. Hashimoto M *et al.* 2010 Planar polarization of node cells determines the rotational axis of node cilia. *Nat. Cell Biol*. **12**, 170–176. (doi:10.1038/ncb2020)
54. Supp DM, Witte DP, Potter SS, Brueckner M. 1997 Mutation of an axonemal dynein affects left–right asymmetry in inversus viscerum mice. *Nature* **389**, 963–966. (doi:10.1038/40140)
55. Jaffe KM *et al.* 2016 *c21orf59/kurly* controls both cilia motility and polarization. *Cell Rep*. **14**, 1841–1849. (doi:10.1016/j.celrep.2016.01.069)
56. Hjeij R *et al.* 2014 *CCDC151* mutations cause primary ciliary dyskinesia by disruption of the outer dynein arm docking complex formation. *Am. J. Hum. Genet*. **95**, 257–274. (doi:10.1016/j.ajhg.2014.08.005)
57. Tarkar A *et al.* 2013 DYX1C1 is required for axonemal dynein assembly and ciliary motility. *Nat. Genet*. **45**, 995–1003. (doi:10.1038/ng.2707)
58. Narasimhan V *et al.* 2015 Mutations in *CCDC11*, which encodes a coiled-coil containing ciliary protein, causes *situs inversus* due to dysmotility of monocilia in the left–right organizer. *Hum. Mutat*. **36**, 307–318. (doi:10.1002/humu.22738)
59. Pennekamp P, Karcher C, Fischer A, Schweickert A, Skryabin B, Horst J, Blum M, Dworniczak B. 2002 The ion channel polycystin-2 is required for left–right axis determination in mice. *Curr. Biol*. **12**, 938–943. (doi:10.1016/S0960-9822(02)00869-2)
60. Schottenfeld J, Sullivan-Brown J, Burdine RD. 2007 Zebrafish *curly up* encodes a *Pkd2* ortholog that restricts left-side-specific expression of *southpaw*. *Development* **134**, 1605–1615. (doi:10.1242/dev.02827)
61. Bisgrove BW, Snarr BS, Emrazian A, Yost HJ. 2005 Polaris and Polycystin-2 in dorsal forerunner cells and Kupffer's vesicle are required for specification of the zebrafish left–right axis. *Dev. Biol*. **287**, 274–288. (doi:10.1016/j.ydbio.2005.08.047)
62. Obara T *et al.* 2006 Polycystin-2 immunolocalization and function in zebrafish. *J. Am. Soc. Nephrol*. **17**, 2706–2718. (doi:10.1681/ASN.2006040412)
63. Field S *et al.* 2011 Pkd1l1 establishes left–right asymmetry and physically interacts with Pkd2.

Development **138**, 1131–1142. (doi:10.1242/dev.058149)

64. Kamura K, Kobayashi D, Uehara Y, Koshida S, Iijima N, Kudo A, Yokoyama T, Takeda H. 2011 Pkd1l1 complexes with Pkd2 on motile cilia and functions to establish the left–right axis. *Development* **138**, 1121–1129. (doi:10.1242/dev.058271)
65. Grimes DT *et al.* 2016 Genetic analysis reveals a hierarchy of interactions between polycystin-encoding genes and genes controlling cilia function during left–right determination. *PLoS Genet*. **12**, e1006070. (doi:10.1371/journal.pgen.1006070)
66. Yoshiba S *et al.* 2012 Cilia at the node of mouse embryos sense fluid flow for left–right determination via Pkd2. *Science* **338**, 226–231. (doi:10.1126/science.1222538)
67. Boskovski MT, Yuan S, Pedersen NB, Goth CK, Makova S, Clausen H, Brueckner M, Khokha MK. 2013 The heterotaxy gene *GALNT11* glycosylates Notch to orchestrate cilia type and laterality. *Nature* **504**, 456–459. (doi:10.1038/nature12723)
68. Hashimoto H *et al.* 2004 The Cerberus/Dan-family protein Charon is a negative regulator of Nodal signaling during left–right patterning in zebrafish. *Development* **131**, 1741–1753. (doi:10.1242/dev.01070)
69. Hojo M *et al.* 2007 Right-elevated expression of charon is regulated by fluid flow in medaka Kupffer's vesicle. *Dev. Growth Differ*. **49**, 395–405. (doi:10.1111/j.1440-169X.2007.00937.x)
70. Vonica A, Brivanlou AH. 2007 The left–right axis is regulated by the interplay of Coco, Xnr1 and derriere in *Xenopus* embryos. *Dev. Biol*. **303**, 281–294. (doi:10.1016/j.ydbio.2006.09.039)
71. Oki S, Kitajima K, Marques S, Belo JA, Yokoyama T, Hamada H, Meno C. 2009 Reversal of left–right asymmetry induced by aberrant Nodal signaling in the node of mouse embryos. *Development* **136**, 3917–3925. (doi:10.1242/dev.039305)
72. Schweickert A, Vick P, Getwan M, Weber T, Schneider I, Eberhardt M, Beyer T, Pachur A, Blum M. 2010 The nodal inhibitor *Coco* is a critical target of leftward flow in *Xenopus*. *Curr. Biol*. **20**, 738–743. (doi:10.1016/j.cub.2010.02.061)
73. Lopes SS, Lourenco R, Pacheco L, Moreno N, Kreiling J, Saude L. 2010 Notch signalling regulates left–right asymmetry through ciliary length control. *Development* **137**, 3625–3632. (doi:10.1242/dev.054452)
74. Marques S, Borges AC, Silva AC, Freitas S, Cordenonsi M, Belo JA. 2004 The activity of the Nodal antagonist *Cerl-2* in the mouse node is required for correct L/R body axis. *Genes Dev*. **18**, 2342–2347. (doi:10.1101/gad.306504)
75. Inacio JM, Marques S, Nakamura T, Shinohara K, Meno C, Hamada H, Belo JA. 2013 The dynamic right-to-left translocation of Cerl2 is involved in the regulation and termination of Nodal activity in the mouse node. *PLoS ONE* **8**, e60406. (doi:10.1371/journal.pone.0060406)
76. Danos MC, Yost HJ. 1996 Role of notochord in specification of cardiac left–right orientation in zebrafish and *Xenopus*. *Dev. Biol*. **177**, 96–103. (doi:10.1006/dbio.1996.0148)
77. Rebagliati MR, Toyama R, Fricke C, Haffter P, Dawid IB. 1998 Zebrafish *nodal-related* genes are implicated in axial patterning and establishing left–right asymmetry. *Dev. Biol*. **199**, 261–272. (doi:10.1006/dbio.1998.8935)
78. Sampath K, Rubinstein AL, Cheng AM, Liang JO, Fekany K, Solnica-Krezel L, Korzh V, Halpern ME. 1998 Induction of the zebrafish ventral brain and floorplate requires cyclops/nodal signalling. *Nature* **395**, 185–189. (doi:10.1038/26020)
79. Lohr JL, Danos MC, Yost HJ. 1997 Left–right asymmetry of a *nodal*-related gene is regulated by dorsoanterior midline structures during *Xenopus* development. *Development* **124**, 1465–1472.
80. Lenhart KF, Lin SY, Titus TA, Postlethwait JH, Burdine RD. 2011 Two additional midline barriers function with midline *lefty1* expression to maintain asymmetric Nodal signaling during left–right axis specification in zebrafish. *Development* **138**, 4405–4410. (doi:10.1242/dev.071092)
81. Meno C *et al.* 1998 *Lefty-1* is required for left–right determination as a regulator of *lefty-2* and *nodal*. *Cell* **94**, 287–297. (doi:10.1016/S0092-8674(00)81472-5)
82. Bisgrove BW, Essner JJ, Yost HJ. 1999 Regulation of midline development by antagonism of lefty and nodal signaling. *Development* **126**, 3253–3262.
83. Meno C, Saijoh Y, Fujii H, Ikeda M, Yokoyama T, Yokoyama M, Toyoda Y, Hamada H. 1996 Left–right asymmetric expression of the TGFβ-family member *lefty* in mouse embryos. *Nature* **381**, 151–155. (doi:10.1038/381151a0)
84. Thisse C, Thisse B. 1999 Antivin, a novel and divergent member of the TGFβ superfamily, negatively regulates mesoderm induction. *Development* **126**, 229–240.
85. Yamamoto M *et al.* 2003 Nodal signaling induces the midline barrier by activating *Nodal* expression in the lateral plate. *Development* **130**, 1795–1804. (doi:10.1242/dev.00408)
86. Nakamura T, Mine N, Nakaguchi E, Mochizuki A, Yamamoto M, Yashiro K, Meno C, Hamada H. 2006 Generation of robust left–right asymmetry in the mouse embryo requires a self-enhancement and lateral-inhibition system. *Dev. Cell* **11**, 495–504. (doi:10.1016/j.devcel.2006.08.002)
87. Wang X, Yost HJ. 2008 Initiation and propagation of posterior to anterior (PA) waves in zebrafish left–right development. *Dev. Dyn*. **237**, 3640–3647. (doi:10.1002/dvdy.21771)
88. Xu B. 2010 Systematic analysis of asymmetric Nodal signaling in the development of zebrafish Left–Right Patterning. Thesis Department of Molecular Biology, Princeton University, Princeton, NJ 08540.
89. Kimmel CB, Ballard WW, Kimmel SR, Ullmann B, Schilling TF. 1995 Stages of embryonic development of the zebrafish. *Dev. Dyn*. **203**, 253–310. (doi:10.1002/aja.1002030302)
90. Brand M *et al.* 1996 Mutations affecting development of the midline and general body shape during zebrafish embryogenesis. *Development* **123**, 129–142.
91. Hammerschmidt M *et al.* 1996 Mutations affecting morphogenesis during gastrulation and tail formation in the zebrafish, *Danio rerio*. *Development* **123**, 143–151.
92. Schier AF, Neuhauss SC, Helde KA, Talbot WS, Driever W. 1997 The *one-eyed pinhead* gene functions in mesoderm and endoderm formation in zebrafish and interacts with *no tail*. *Development* **124**, 327–342.
93. Strahle U, Jesuthasan S, Blader P, Garcia-Villalba P, Hatta K, Ingham PW. 1997 *one-eyed pinhead* is required for development of the ventral midline of the zebrafish (*Danio rerio*) neural tube. *Genes Funct*. **1**, 131–148. (doi:10.1046/j.1365-4624.1997.00010.x)
94. Nasevicius A, Ekker SC. 2000 Effective targeted gene 'knockdown' in zebrafish. *Nat. Genet*. **26**, 216–220. (doi:10.1038/79951)
95. Agathon A, Thisse B, Thisse C. 2001 Morpholino knock-down of antivin1 and antivin2 upregulates nodal signaling. *Genesis* **30**, 178–182. (doi:10.1002/gene.1059)
96. Saude L, Woolley K, Martin P, Driever W, Stemple DL. 2000 Axis-inducing activities and cell fates of the zebrafish organizer. *Development* **127**, 3407–3417.
97. Shih J, Fraser SE. 1996 Characterizing the zebrafish organizer: microsurgical analysis at the early-shield stage. *Development* **122**, 1313–1322.
98. Krauss S, Concordet JP, Ingham PW. 1993 A functionally conserved homolog of the *Drosophila* segment polarity gene *hh* is expressed in tissues with polarizing activity in zebrafish embryos. *Cell* **75**, 1431–1444. (doi:10.1016/0092-8674(93)90628-4)
99. Schulte-Merker S, van Eeden FJ, Halpern ME, Kimmel CB, Nusslein-Volhard C. 1994 *no tail* (*ntl*) is the zebrafish homologue of the mouse T (*Brachyury*) gene. *Development* **120**, 1009–1015.
100. Amack JD, Yost HJ. 2004 The T box transcription factor no tail in ciliated cells controls zebrafish left–right asymmetry. *Curr. Biol*. **14**, 685–690. (doi:10.1016/j.cub.2004.04.002)
101. Bisgrove BW, Essner JJ, Yost HJ. 2000 Multiple pathways in the midline regulate concordant brain, heart and gut left–right asymmetry. *Development* **127**, 3567–3579.
102. Chin AJ, Tsang M, Weinberg ES. 2000 Heart and gut chiralities are controlled independently from initial heart position in the developing zebrafish. *Dev. Biol*. **227**, 403–421. (doi:10.1006/dbio.2000.9924)
103. Halpern ME *et al.* 1997 Genetic interactions in zebrafish midline development. *Dev. Biol*. **187**, 154–170. (doi:10.1006/dbio.1997.8605)
104. Feldman B, Concha ML, Saude L, Parsons MJ, Adams RJ, Wilson SW, Stemple DL. 2002 Lefty antagonism of Squint is essential for normal gastrulation. *Curr. Biol*. **12**, 2129–2135. (doi:10.1016/S0960-9822(02)01361-1)